Reprinted from Applied Optics, Vol. 24, page 2313, August 1, 1985
Copyright © 1985 by the Optical Society of America and reprinted by permission of the copyright owner.

Optical time-domain reflectometer specifications and performance testing

Bruce L. Danielson

From a researcher's as well as a user's point of view, it is highly desirable to adopt a common basis for specifying optical time-domain reflectometer performance parameters. This paper proposes some procedures and test methods which permit these devices to be characterized in a consistent way. Passive test fixtures are also described which may facilitate measurements of dynamic range and other reflectometer properties.

I. Introduction

Since its development less than ten years ago,[1,2] the optical time-domain reflectometer (OTDR) has established itself as one of the more versatile instruments for characterizing optical fibers and fiber installations. Applications of this device, which have been reported in the literature, include measurements of splice loss,[3–5] connector insertion loss,[6] coupler branching ratios,[7] fiber attenuation,[8] microbending loss,[9] diameter fluctuations,[10] fiber and cable length,[11] differential modal scattering,[12] mode-mixing lengths,[13] nonlinear scattering gain,[14] and mode conversion at joints.[15] The locations and identification of defects[11] and other system diagnostics[16] are also important applications. Further evidence of the utility of the OTDR is provided by the fact that there are approximately twenty manufacturers currently engaged in producing various types of this device intended for both single-mode and multimode use.[17]

For comparison and specification purposes it is desirable to have some kind of common testing methodology for evaluating the measurement capabilities of these instruments. Unfortunately, the technical literature is replete with different specification terminologies and test methods. In the present paper, we will attempt to review some of these differences and explore a few possibilities for generating consistent values for the more important OTDR performance parameters. Some specific measurement techniques and test devices are described which may be useful in this connection.

The author is with U.S. National Bureau of Standards, Electromagnetic Technology Division, Boulder, Colorado 80303.

Received 26 April 1985.

II. Background

The basic principles of operation of a conventional OTDR are illustrated in Fig. 1. A short duration pulse of optical radiation (20–2000 nsec) is launched into a test fiber via a directional coupler. The all-fiber coupler is the most common, although bulk optics (lenses and beam splitter) may also be used. The output of the directional coupler (R/T port) serves to both receive the backscattered radiation and transmit the probe pulse in the forward direction. The R/T port may consist of a connecterized termination or a micropositioner and jig which accepts a bare fiber. Backreflected radiation from the test fiber is detected, processed, and finally displayed on an oscilloscope screen or recorder of some sort. The output signal response as a function of distance along the fiber is often referred to as a signature, since it is a characteristic that can be identified with a particular fiber or fiber system.

Two distinct types of feature are observed on the signature. First, reflections will arise from discontinuities such as small bubbles in the fiber and Fresnel reflections from breaks, couplers, and certain types of splice. Second, a continuous return is generated due to Rayleigh scattering of the probe pulse traveling in the forward direction. This type of scattering, which is approximately isotropic and proportional to the inverse fourth power of the optical wavelength, is always present when radiation propagates in amorphous materials. It arises from dipole moments induced in the transmitting medium by refractive-index fluctuations and, to a lesser extent, inhomogeneities in the dopant concentration. Due to the wide dynamic range of signal amplitude encountered in many applications, as well as convenience in interpretation, the preferred signature display is semilogarithmic. For example, the logarithm of the backscattered power (optical decibels) may be displayed vs linear distance (meters). Figure 2 illustrates a typical signature along with some of the features

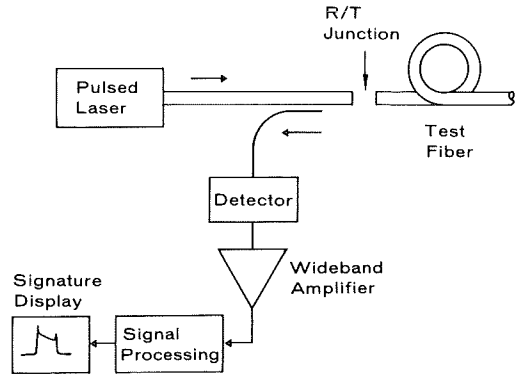

Fig. 1. Schematic representation of a conventional OTDR. A common port (R/T junction) is used to transmit the probe pulse and receive the backscattered optical signal.

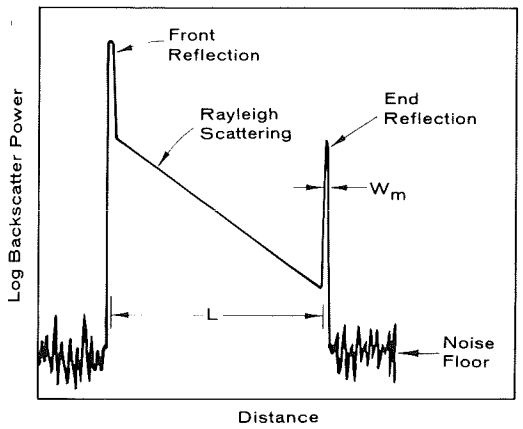

Fig. 2. Example of a logarithmic signature for a uniform fiber. Indicated quantities are used in characterizing the OTDR (see text). The noise floor is defined to be the point where the extrapolated SNR is one. The quantity W_m is the FWHM at a point −3 dB (optical) from maximum.

normally observed from a test fiber. The indicated noise floor P_n is defined as the optical power level (injected at the R/T port), which is equal in magnitude to the rms noise; i.e., the displayed SNR is equal to 1 at this point.

The theory of scattering in optical waveguides has been discussed by a number of authors.[18,19] From these references it follows that the Rayleigh backscattered power $P_b(x)$ as a function of distance x along the lightguide, whose transmission properties are independent of x, may be cast in the form

$$P_b(x) = P_0 WS \exp(-2\alpha_T x). \tag{1}$$

P_0 is the peak optical power (watts) in the injected probe pulse, W is its duration (seconds) and is assumed to have a rectangular shape, and α_T is the total attenuation rate (m^{-1}) of the waveguide. For the multimode case, the backscatter factor $S(W/J)$ is given by

$$S = \frac{3\alpha_s g(\text{N.A.})^2 v}{16 n_1^2 (g+1)}. \tag{2a}$$

Here α_s is the Rayleigh scattering coefficient (m^{-1}), v is the pulse group velocity (m/sec), N.A. is the numerical aperture, n_1 is the on-axis index of refraction, and g is the index profile parameter.[20] The corresponding equation for a step-index single-mode fiber is[21]

$$S = \frac{3}{16}\alpha_s v \left(\frac{\lambda}{\pi n_1 \omega_0}\right)^2, \tag{2b}$$

where $2\omega_0$ is the mode-field diameter [the near-field intensity varies as $\exp(-2r^2/\omega_0)$ as a function of radius r], and λ is the wavelength. The backscatter factor is the crucial fiber parameter which determines the level of optical power that is returned to the R/T port for any test fiber.

From Eq. (1) we see that the fiber loss may be inferred from the slope of the display of the logarithm of the power vs distance. The total fiber loss A_L between $x = 0$ and $x = L$ is

$$A_L = -5 \log \left[\frac{P_b(L)}{P_b(0)}\right] \quad \text{dB (one-way loss)} \tag{3}$$

using Eq. (1) and the identity $A_L = 10\alpha_T L \log e$. This can be compared to the backscattered power ratio relative to the same two points:

$$\text{Backscatter power loss} = -10 \log \left[\frac{P_b(L)}{P_b(0)}\right] \quad \text{dB (optical).} \tag{4}$$

The factor of 2 difference between decibels (one-way loss) in Eq. (3) and decibels (optical) in Eq. (4) arises from the fact that the observed radiation must travel in the forward direction to the scattering point and then return in the backward direction to the receiver and so is attenuated twice. In this connection we also note that the SNR of signal output from a detector is customarily expressed in terms of electrical decibels.[21] Since electrical power is proportional to the square of optical power (in square-law detectors), we have for the maximum SNR in this case

$$\text{SNR} = 20 \log \left[\frac{P_b(0)}{P_n}\right] \quad \text{dB (electrical).} \tag{5}$$

The decibel scales in Eqs. (3), (4), and (5) are numerically different, and occasional confusion has resulted from failure to observe the distinction between them. In the discussion which follows, we will state explicitly which decibel scale is being referred to.

III. OTDR Performance Parameters

A number of instrumental characteristics may be used in OTDR specifications. These include logarithmic display accuracy, transmitter pulse energy and repetition rate, environmental stability, receiver saturation levels, receiver sensitivity in dB/m, overload recovery time, and coupler cross talk isolation. Although any or all of these may be of concern in specific applications, we will restrict the present discussion to what are probably the most important of the performance criteria. These are dynamic range, resolution, fault location accuracy, and averaging time.

Obviously, the first requirement for uniform specifications is in the area of terminology. There are myriad quite different definitions currently in use both in the research literature and in commercial specifications. We will review some of these and also mention our own

preferences. The latter are, to a certain extent, arbitrary.

A. Dynamic Range

The dynamic range is kind of a figure of merit used to indicate the measurement capabilities of an OTDR.[22–25] A good discussion of the different notations and associated measurement problems has been given by Philen *et al.*[26] The dynamic range is usually expressed, in decibels, in terms of some maximum optical power in the system P_{max} to a reference minimum optical power P_{min} in a relationship of the form $K \log(P_{max}/P_{min})$. Various possibilities have been used for K, P_{max}, and P_{min}. For example, P_{max} may be the maximum observed backscattered power, or the probe pulse optical power injected into either the directional coupler or the test fiber at the R/T port. For the end-detection dynamic range P_{max} is taken to be the power reflected from a mirror-surface fiber break. A similar notational diversity exists for the lower power limit. P_{min} may represent the noise floor P_n or some other working-value power level where nonlinearities or noise result in errors exceeding preset limits. Signal levels can be determined at either the detector (after traversing the coupler) or the R/T port. The constant K depends on the type of dynamic range specified; $K = 5$ for a one-way loss, $K = 10$ for a two-way loss or decibel (optical), and $K = 20$ for a dynamic range put in terms of electrical units. (This usage is not common.)

Although any of these definitions can be justified, in the present work we will adopt the formulation given by Hartog[27] and others. Here the dynamic range D is given in terms of the maximum possible measurable one-way loss as follows:

$$D = 5 \log \left[\frac{P_b(0)}{P_n}\right] \quad \text{dB (one-way loss)}, \tag{6}$$

where $P_b(0)$ is the backscatter signal at the input end of a reference test fiber (to be described in detail in the next section), and P_n is the noise floor after signal averaging. This definition is convenient from several standpoints. It can be easily measured in an unambiguous way; it has a meaningful physical significance; and access to the internal components of the OTDR is not required. Also, the dynamic range defined in Eq. (6) is numerically equal to twice the maximum SNR (decibel optical) obtained from the reference fiber. Other commonly used terms can be expressed relative to this dynamic range definition. For example, the end-detection dynamic range $5 \log[P_0 R/P_n]$ with an end reflectance r is

$$D + 5 \log \left[\frac{r}{WS}\right] \quad \text{dB (one-way loss)},$$

and the signal acquisition range expressed in terms of the power transmitted through a short fiber, $10 \log[P_0/P_n]$, is

$$2D + 10 \log [WS] \quad \text{dB (optical)}.$$

B. Spatial Resolution Limit

Here again we have an abundance of definitions, but ideally resolution should denote the ability of the reflectometer to distinguish between defects or fiber perturbations which occur in close proximity. A relation which is carried over from radar usage defines resolution as $Wv/2$. Marcuse[28] has shown that this is appropriate in cases where the minimum resolvable defect separation is determined by the probe pulse duration, and that pulse is assumed to be rectangular in shape. In some situations the resolution may be limited by certain instrumental effects such as the postdetection bandwidth or digital sampling intervals. For this reason we prefer a working definition of the spatial resolution limit R as a measure of the smallest spacing of reflecting elements which can just be resolved and whose nominal value is given by

$$R = (W_m v)/2 \quad (m), \tag{7}$$

where W_m is the full width at half-maximum (FWHM) of a discrete reflection as observed on the OTDR display. On the usual logarithmic scale, this corresponds to the pulse width at the −3-dB (optical) level. Some reflections, such as the 4% Fresnel return from a perfect fiber break, may be sufficiently large to saturate the receiver, and obviously measurements must not be made under these conditions. Also the definition in Eq. (7) assumes no pulse broadening due to fiber dispersion effects. In most cases of interest this poses no problems. It should also be emphasized that Eq. (7) is an operational definition, and in fact it may not be possible to distinguish certain types of nonreflecting faults using this criterion.[29]

From a comparison of Eqs. (1), (6), and (7) we see that there is a trade-off in resolution limit and dynamic range. The backscatter signal level is proportional to the probe pulse duration, but increasing this pulse width degrades the resolution. An additional factor to consider is the receiver noise bandwidth, which normally varies inversely with W. Therefore, it is to be expected that optimum resolution and maximum dynamic range will occur under different operating conditions.

C. Fault Location Accuracy

As the name implies, OTDR measurements are conducted in the time domain. However, the scale of interest is usually not time but distance along the fiber or cable. Conversion of time to distance is accomplished through the relation $x = vt/2$, and this requires knowledge of the group velocity or, equivalently, the group index of refraction $N = c/v$ with c the velocity of light. For the cable situation, the excess length of the fiber over that of the cable is implicitly contained in N.

Fault location, or range, accuracy refers to the ability of the OTDR to locate spatially a discrete signature feature, in meters, when the group index or group velocity of the lightguide or cable is known. Some authors consider this term to be synonymous with resolution as given above,[30] but there can be significant differences between the two definitions. Several types of uncertainty contribute to errors in range determination.

Systematic errors may occur in the reflectometer time determinations and in the process of converting that time interval into distance information. Measurement precision, or repeatability, is largely a function of the rise time τ of the probe pulse. It can be shown[31] that the magnitude of this error is approximately τ/SNR.

The best way to determine the end location accuracy for a given OTDR is by means of an appropriate statistically analysis of repeated measurements on a fiber of known length, group index, and end reflectance.

D. Averaging Time

Practically all OTDRs have some sort of postdetection signal averaging device to improve the displayed SNR. The most common types of averager are the boxcar integrator, a single-point analog device, and the digital multichannel averager. The last type is much more efficient since many points are sampled on each pulse.[32] For stationary noise processes, the linear SNR as well as the linear measured dynamic range can be improved by a factor of the square root of the averaging time.

The averaging time will be a function of the number of displayed points, averaging technique, and fiber length. The length dependence arises from the fact that the source repetition rate must be limited to $2L/v$ pps to prevent successive signals from overlapping.

For comparison purposes, SNR or the dynamic range can be scaled to a constant data-collection time. This averaging time may be an important practical consideration from the operator's standpoint, but its determination presents no essential difficulties and will not be considered further.

IV. Reference Test Conditions

We have taken the position that the most convenient way to characterize the OTDR is through observation and analysis of the displayed response of the reflectometer to a reference test fiber. The signature of a properly chosen fiber can completely determine the performance parameters previously discussed. For meaningful and reproducible results the standard reference test fiber must have well-characterized transmission properties including a known backscatter response, and the measurements must be made under specified experimental conditions. We will now discuss some of these requirements.

A. Reference Test Fiber

At the present time there is no unique standard lightguide we can adopt for testing purposes. The Electronic Industries Association (EIA) has recently promulgated a list of standard optical waveguide material classes and preferred sizes, which can serve as possible candidates. These are summarized in Tables I and II.[33] The material classes and preferred sizes for single-mode fibers (Class IV) have not be determined at the present time. The International Telegraph and Telephone Consultative Committee (CCITT) only recognizes two standard fiber types. They are the 50/125 multimode and single mode with 9–10-μm mode-field diameter and 125-μm o.d. Attenuation rates and scattering losses are not included in any of these specifications.

Table I. Multimode Optical Waveguide Fiber Material Class Standards

Class	Index	Profile parameter g	Core material[a]	Cladding material[a]	Jacket material
I*a*	Graded	$3 > g > 1$	Glass	Glass	
I*b*	Quasi-step	$10 > g > 3$	Glass	Glass	
I*c*	Step	$g > 10$	Glass	Glass	
II*a*	Step	$g > 10$	Glass	Plastic	
II*b*	Step	$g > 10$	Glass	Plastic	Plastic
III	Step	$g > 10$	Plastic	Plastic	

[a] The term glass refers to an amorphous material consisting of metallic oxides.

Table II. Preferred Sizes of Optical Waveguide Fibers

Material class	Core diameter (μm)	Outside (clad) diameter (μm)	Numerical aperture (N.A.)
I	50	125	0.19–0.25
I	62.5	125	0.27–0.31
I	85	125	0.26–0.29
I	100	140	0.25–0.30
I	200	250	0.14–0.16
II	200	To be specified	To be specified
II	400	To be specified	To be specified
III	To be specified	To be specified	To be specified

All the recommended classes and sizes include fibers with a large variation in transmission properties and, therefore, will exhibit a large variation in Rayleigh backscatter levels. This can be seen from and examination of Eq. (1), which states that the initial scattered signal is equal to the product of the backscatter factor and the energy P_0W, which is coupled into the test fiber. Both these quantities are strongly dependent on the fiber transmission properties. For multimode fibers the coupled energy is proportional to the number of possible bound modes M given by[34]

$$M = \frac{g}{2(g+2)}\left(\frac{2\pi a}{\lambda}\right)^2 (\text{N.A.})^2. \tag{8}$$

In the single-mode case the coupling efficiency is determined for the most part by the test-fiber mode spot size. The precise coupling efficiency cannot be predicted accurately without detailed knowledge of the radiance properties of the effective source at the OTDR output port. Nevertheless, under certain circumstances, the combined effect of parameter excursions in M, Eq. (8) and S, Eq. (2) on the backscattered power implies a variation of as much as 12 dB in signal level for multimode fibers within a given waveguide material class. Therefore, if we are to use the maximum power level $P_b(0)$ in dynamic range specifications, well-characterized reference fibers are required. The most important properties of the reference fiber which must be fixed are those that determine the magnitude of the backscatter level. These are core diameter, numerical aperture, profile parameter, and backscatter factor for multimode fibers and mode-field diameter and backscatter factor for single-mode fibers.

B. Wavelength

Most multimode OTDRs are designed to operate at 820, 850, or 1300 nm. Since backscattering levels are proportional to the inverse fourth power of the wavelength λ, the backscatter factor must be scaled by this factor if measured at one wavelength and used in testing an OTDR operating at a different wavelength. A backscatter factor of 150 W/J at 850 nm corresponds to 173 W/J at 820 nm and 27 W/J at 1300 nm. Coupling efficiencies are also somewhat wavelength dependent.

C. Measurement Conditions

Usually OTDRs are used with overfill launching conditions (all modes excited). A mandrel wrap mode filter[36] will generally improve agreement with the cutback method of measuring attenuation but at the expense of a several-decibel loss in backscatter signal level. In performance testing applications there seems to be little justification in using a mode filter. A mode stripper[20] is used to remove the power propagating in the cladding which occurs under overfill launch conditions. For very short fiber lengths, e.g., 1 m, both forward-propagating and backscattered radiation in the cladding may be significant. This source of stray radiation is usually negligible after a few tens of meters due to the high loss associated with cladding modes. Also, many modern fibers have lossy high-index coatings which act as effective mode strippers. Although backscatter in the cladding is unlikely to be a problem, prudence suggests a check to establish this fact.

V. Test Methods

There are two principal methods for testing the capabilities of an optical time-domain reflectometer. These can be classified as active and passive techniques. Active methods require additional test equipment to measure separately the properties of the OTDR source and receiver. They give a more complete characterization of the reflectometer laser components but do not directly measure most of the performance parameters of interest as we have defined them. For example, probe pulse power, time duration, and repetition rate can be measured by means of a short reference fiber coupled to a calibrated detector. The receiver linearity and noise floor can be evaluated by injecting into the R/T port optical pulses of known amplitude from an optical signal generator. Devices specifically designed for this purpose are available commercially. On the other hand, passive methods rely on reference fibers of some sort to generate a test signal which is then evaluated on the OTDR display. Dynamic range, resolution, and fault location accuracy may be obtained directly in this way. We will consider a few possible passive approaches.

A. Long Fiber

Of all the methods of obtaining OTDR dynamic range, the simplest, as well as the most commonly used, involves interpretation of the backscattered signal from a long test fiber. The long fiber itself need not be a standard reference fiber as long as even a fairly short reference fiber is available to establish the necessary normalization of the backscattered signal at $x = 0$.

If the long test fiber has insufficient length to generate a continuous backscatter response which extends to the noise floor, the observed slope may be extrapolated for this purpose. There is one possible drawback to this extrapolation procedure. If the zero-signal level is improperly set, display nonlinearities occur near the noise floor, and the noise floor itself is displaced. These zero-level offsets may derive from such sources as base line tilt due to ac coupling or incorrect bias levels in the logarithmic amplifier. Since these effects are apparent only for low-level signals, they will go unnoticed unless the loss signature extends to the noise level. A complete signature involves a fiber whose loss in decibels equals or exceeds the dynamic range. This requirement may necessitate a fairly long fiber in some cases. For example, an OTDR dynamic range of $D = 47$ dB (one-way loss) has been reported in a multimode system[37] and 41 dB in a single-mode system.[38]

The resolution in Eq. (7) can be inferred from the end Fresnel reflection as shown in Fig. 2. The test fiber end may be inserted in a partially index-matched fluid to attenuate this signal feature to a convenient level.

Evaluation of the fault location accuracy may be accomplished by comparing the apparent reference fiber length indicated on the signature display with the actual length measured by mechanical means. The group velocity, or the group index, must also be determined independently. This can be done by frequency domain or time-of-flight measurements on a fiber whose length is known.

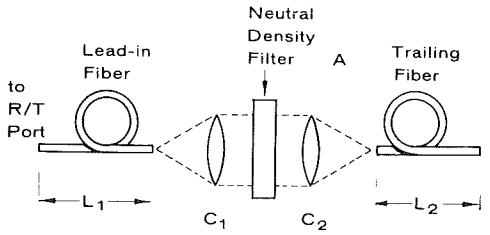

Fig. 3. Test fixture consisting of a neutral density filter with attenuation A placed between collimating lenses C_1 and C_2. The filter may be one of a series which is mounted on a rotating wheel.

B. Fiber and Attenuator

The requirement on fiber length can be mitigated considerably by means of an arrangement shown in Fig. 3.[39] Here a series of calibrated neutral density filters is inserted between two reference fibers. For convenience, the various filters can be mounted on a suitable wheel. Linearity as well as dynamic range may be deduced from the resultant response, as shown in Fig. 4. Careful design is required to prevent the emanation of large reflections from the region between the two fibers. A related technique has been reported by Kurki and Viljanen.[23]

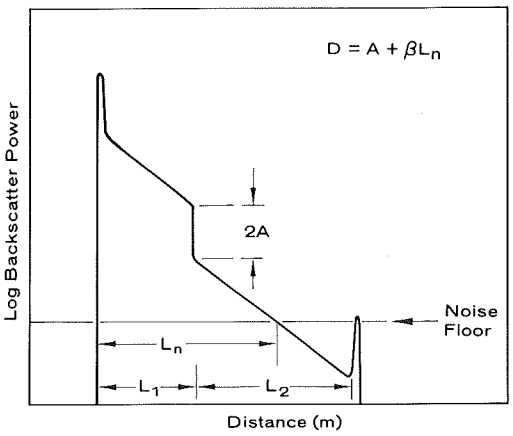

Fig. 4. Schematic OTDR display for the test fixture shown in Fig. 3. The dynamic range D is given by the one-way loss to the noise floor. The quantity β is the one-way fiber attenuation rate (dB/m).

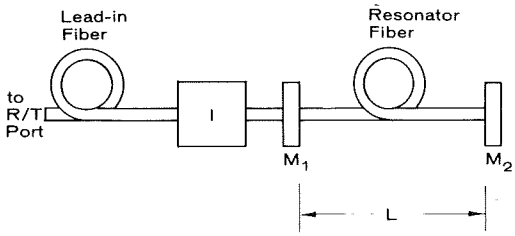

Fig. 5. Recirculating delay line test fixture. The resonator is formed by mirrors M_1, M_2, and length L of graded-index fiber. An isolator I is used to suppress the initial unwanted reflection from M_1. The lead-in fiber generates the reference backscatter signal.

C. Recirculating Delay Lines

A well-characterized backscatter signature may also be generated with certain types of passive delay fixture constructed from recirculating fiber delay lines. These devices fall into two categories. The first returns a series of pulses to the receiver, each being a replica of the probe pulse. In other structures only Rayleigh scattering is returned. Both types can be used to provide a convenient reference response. Since these test fixtures have not been described elsewhere, we will describe them here in some detail.

The principle of operation of the shuttle-pulse test fixture is illustrated in Fig. 5. A recirculating delay line is formed by two mirrors, $M1$ and $M2$, and ~50 m of graded-index fiber. Cohen[40] originally used this type of structure to investigate pulse broadening effects in relatively short lengths of fiber. Also, Marcuse[41] has discussed, from a theoretical point of view, how losses in these devices approach an equilibrium value. In the present application the probe pulse from the OTDR is injected into this resonator from ~100 m of lead-in reference fiber which establishes the backscatter level required for the dynamic range measurement. The isolator I suppresses the initial large reflection from the front surface of $M1$. Once inside the resonator, the pulse of optical radiation shuttles back and forth between the two mirrors. The physical length of the pulse of radiation, $x = vW$, is much smaller than the optical path length between the mirrors, so that no interference effects need be considered. Each time the pulse impinges on the mirror $M1$ from the right, some of the radiation is transmitted back to the OTDR. The series of pulses produces a kind of picket fence signature. This type of reference signature generator can be built to produce pulses of controllable magnitudes which vary from saturation levels down to levels comparable to the noise in the receiver. It is not difficult to obtain approximately constant loss for successive pulses.

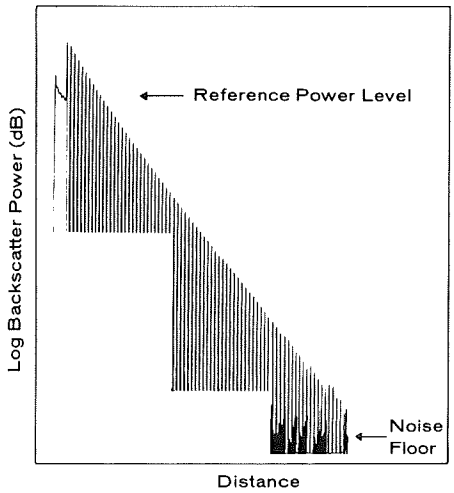

Fig. 6. Composite signature from the text fixture shown in Fig. 5. The reference power level from a standard fiber and the noise floor determine the dynamic range of the OTDR. The loss per pulse is ~0.63 dB (optical). Nonlinearities are due to instrumental effects.

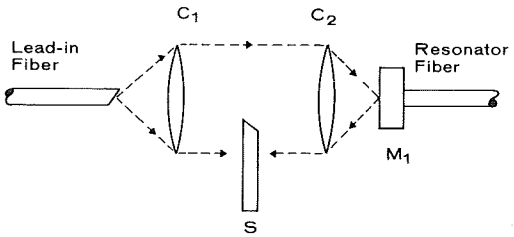

Fig. 7. Isolator used in the test fixture of Fig. 5. A slit S is placed in the beam produced by the collimated lenses C_1 and C_2. The upper half of the beam from the lead-in fiber is imaged onto the mirror M_1, and the reflection is stopped by the slit. The end of the lead-in fiber is beveled to eliminate the Fresnel reflection at that point.

A typical test fixture signature is shown in Fig. 6, which is actually a composite of three backscatter scans taken with different receiver gain settings. For this case, the mirror $M1$ had a nominal reflectance of 98%, and the mirror $M2$ was totally reflecting. Devices have been built with the loss per pulse as small as 0.5 dB (optical), equivalent to a one-way loss of 0.25 dB. The isolator for minimizing the initial $M1$ reflection is shown in Fig. 7. It consists of a simple stop, in the form of a slit, which attenuates one-half of the beam propagating in the forward direction. Ray tracing, as indicated by arrows, illustrates the principle of operation. The image focused on the input end of the resonator fiber is not azimuthally symmetrical, but, due to coupling

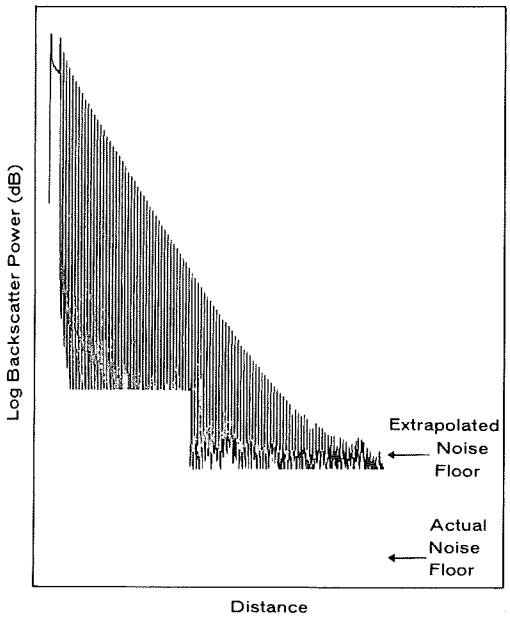

Fig. 8. Test fixture signature showing the effect of a zero-offset error. Arrows indicate the apparent noise floor extrapolated from large signals, and the actual noise floor with the zero level correctly set.

among degenerate modes, the flux symmetry is quickly established. The backscattered power under these conditions occupies the full numerical aperture of the fiber, and a 3-dB loss is again encountered as the radiation traverses the isolator in the reverse direction. Another source of unwanted reflection occurs at the remote end of the lead-in fiber. This Fresnel return can be eliminated by grinding and polishing the end of the fiber at an angle of ~10°.

The significance of the structure on the test fixture signature is as follows. The dynamic range in Eq. (6) is obtained from the total loss between the reference backscatter power level and the noise floor. This is done by the simple process of counting the number of pulses between these signal levels and multiplying by the constant predetermined loss per pulse. Also, the resolution from Eq. (7) may be obtained from any of the indicated pulse widths. Finally, the length of the two fibers is carefully measured with steel tape, and the group velocity is determined from time-of-flight measurements using a digital delay generator as discussed above. This procedure calibrates the horizontal scale for checking the location accuracy of the OTDR.

The effect of zero-signal offsets is shown in Fig. 8. Pronounced small signal nonlinearities are evident. The apparent noise floor and the noise floor for a correctly set null level are shown by arrows. Nonlinearities are also observed at high signal levels. These are due to signal overload effects in the receiver.

Figure 9 shows the SNR for a pulse in the vicinity of $n = 72$. A display such as this allows for a convenient comparative evaluation of OTDR capabilities under maximum possible operating distances.

A second type of recirculating-delay-line test fixture is shown in Fig. 10. This geometry returns only the backscattered radiation to the R/T port. A lead-in

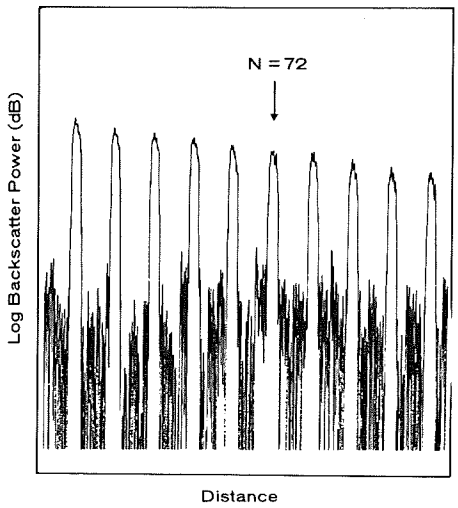

Fig. 9. Expanded-scale test-fixture signature in an interval where the SNR is easily estimated. The seventy-second pulse is indicated by the arrow.

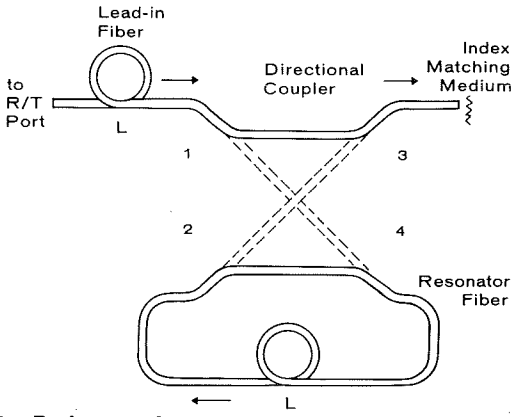

Fig. 10. Backscatter-delay-line test fixture. In this case the lead-in and resonator fiber are both of length L. The probe pulse travels in the direction of the arrows and the backscatter signal in the opposite direction.

reference fiber of length L is connected to a directional coupler which has two of the ports joined to form a closed loop also of length L. Single-mode versions of similar devices have been described by Newton *et al.*[42] The probe pulse energy is coupled into the loop from ports 1 and 4. This pulse continues to circulate in the loop via ports 2 and 4. A complete analysis of the backscatter response of this device will be given elsewhere. For the present, we simply note that, if n is the number of complete circuits around the loop and if we assume a probe pulse of unit energy, the signature assumes the form

$$P_b(x) = S \exp(-2\alpha_T x) \qquad x \le L \tag{9}$$

corresponding to the lead-in fiber, and

$$P_b(x) = (1+n)K_{14}^2 K_{34}^n S \exp[-2\alpha_T(x+L)] \qquad x > L. \tag{10}$$

Here K_{14} and K_{34} represent the fractional transmission loss between, respectively, ports 1 and 4, and 3 and 4. We have also assumed that losses are the same in the

forward and backward directions. Equation (10) takes into account backscatter contributions returned to the R/T port from the nth circuit of the probe pulse propagating in the forward (clockwise direction), and in addition the n components of the backscattered radiation circulating in the opposite direction. With the present assumptions, all these contributions have the same magnitude. A desktop-computer-generated signature is shown in Fig. 11 for the case of a 3-dB coupler with no excess insertion loss, i.e., $K_{14} = K_{34} = 0.5$.

The main attraction of the directional coupler test fixture is that the signature from fairly short fibers (1 km or so) can simulate an infinitely long fiber. The chief problem, at least for multimode operation, is that many couplers have mode-dependent coupling constants. For example, with fused biconical taper couplers, ports 2 and 4 tend to couple low-order modes preferentially, and the high-order modes are favored for coupling through ports 1 and 4. This fact complicates the signature interpretation.

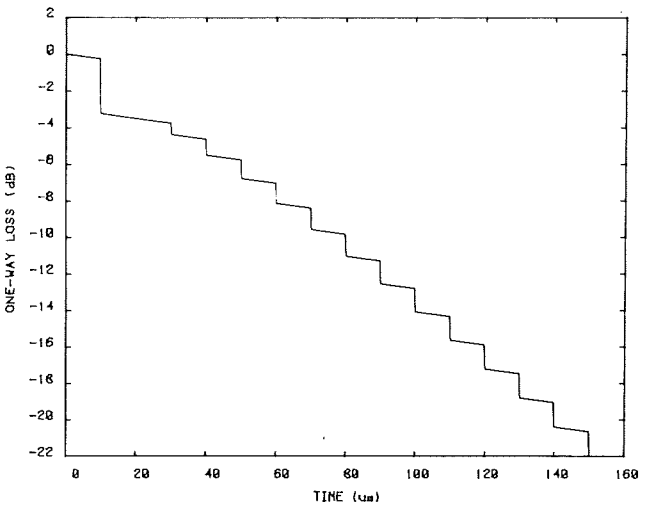

Fig. 11. Simulated backscatter signature from the test fixture shown in Fig. 10. We have assumed $L = 1$ km and a fiber loss of 0.5 dB/km (one-way).

VI. Backscatter Factor Measurements

Accurate measurements of the backscatter factor are necessary for the proper characterization of any standard reference fiber. Several methods for estimating the magnitude of this quantity are possible. The simplest, of course, is obtained by calculation of Eq. (2) using known values of the waveguide parameter. Nominal values of the numerical aperture and profile parameter are available from the manufacturer. The Rayleigh scattering coefficient can be obtained by means of calorimetric methods[43] or from a plot of total fiber loss vs the inverse fourth power of the wavelength, as suggested by Inada.[44] For most high-quality optical fibers, Rayleigh scattering is the dominant attenuation mechanism.

Neumann[45] has suggested an experimental method for determining the backscatter factor. This approach involves measuring the ratio of the optical power returned from the end of a lightguide due to the Fresnel reflection $P_r(L)$ to the Rayleigh backscatter power at the same point $P_b(L)$. This ratio is related to S according to the equation

$$S = rW\frac{P_b(L)}{P_r(L)} \tag{11}$$

with r the reflectance of the glass–air interface. The magnitude of r for a perfect mirror surface perpendicular to the fiber axis is given by the well-known relation

$$r = \left(\frac{n_1 - 1}{n_1 + 1}\right)^2, \tag{12}$$

where n_1 is the average index of refraction of the core material. The main problem with measuring S in this way has to do with the difficulty in obtaining precisely normal and perfectly cleaved reflecting surfaces on the fiber end.

Probably the most accurate method of measuring S has been described by Gold and Hartog.[46] Although their treatment pertained to single-mode lightguides, the method is applicable to multimode guides as well. They simultaneously measure the ratio of scattered and transmitted power from a test fiber. The transmitted power is suitably attenuated with calibrated neutral density filters so that the magnitude is comparable with the backscattered power levels. This method, and modifications thereof, does not require detectors calibrated absolutely, i.e., in terms of watts. The authors found good agreement between the theoretical relationships for S (for single-mode fibers) and experiment.

VII. Noise Floor Measurements

According to our stated approach, measurement of minimum detectable power, or noise floor, involves comparison of a known optical signal with the rms noise amplitude estimated directly from the OTDR signature. The location of the rms noise level on a logarithmic display (Fig. 12) may be determined by noting that, for Gaussian noise processes, ~16% of the sampled noise amplitudes will lie above the rms value. The sampled noise amplitudes are assumed to be spaced by at least an amount equal to the reciprocal of two times the system bandwidth, according to the Shannon sampling theorem. The value of P_n may also be estimated from the peak noise excursion as follows. For a population of ~100 sampled time intervals, the rms noise amplitude lies 3.9 ± 0.6 dB (optical) below the maximum value. The limits here represent one standard deviation. This relationship can be established without difficulty using Monte Carlo methods and a desktop microcomputer.

VIII. Reference Fibers

There are two possible alternatives for reference fibers. They may be paper standards which specify appropriate transmission and scattering properties or artifact standard reference materials (SRMs) consisting of selected types of fiber intended for calibration and performance evaluation purposes.

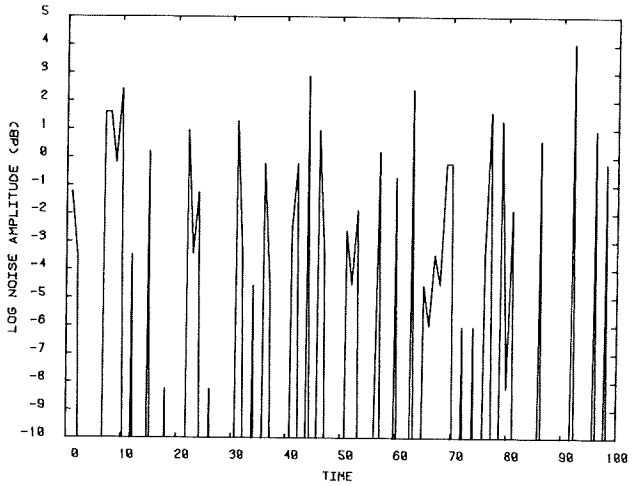

Fig. 12. Simulated Gaussian noise sampled at 100 intervals. The rms amplitude is taken to be the 0-dB level. Approximately 16% of the amplitudes are larger than this value. Also, we may estimate the rms value as 3.9 dB (optical) below the observed maximum value. This latter estimate is within 0.6 dB of the true rms value 68% of the time.

The use of standard reference materials for calibrating analytic instruments is not a novel concept. In fact, at the present time the National Bureau of Standards (NBS) issues over 1000 SRMs, which are produced in quantity for use in improving measurement science.[47,48] Examples of these materials include crystals for use in electron paramagnetic resonance measurements for determining the number of active paramagnetic centers in a test sample, glass filters with verified transmittance for spectrophotometric applications, and metallic specimens for use in calibrating and checking the performance of microhardness testers. Special reference materials of this sort may also be produced or certified by other standard groups or organizations.

We have seen that the properties which need to be specified for either a paper standard or SRM include numerical aperture, backscatter factor, attenuation index profile parameter and core diameter for multimode fibers, and mode-field diameter, attenuation, and backscatter factor for single-mode fibers. In addition, any SRM should have carefully documented quality control to insure batch-to-batch reproducibility and acceptable cost and availability. We believe that a number of commercially available optical fibers could fulfill these requirements.

IX. Summary

In this paper we have offered a few proposals for evaluating OTDR capabilities in a uniform way. The first step in this direction must be an effort to achieve a consensus on terminology, and we have offered what we feel are the most appropriate operational definitions for the quantity's dynamic range, resolution, and fault location accuracy. From the standpoint of device comparison, it is desirable to specify a dynamic range in terms of the OTDR response to a standard reference fiber. As long as the properties of the reference fiber are agreed on, those properties may be arbitrary within broad limits within a given class of fibers.

Some test procedures and devices have also been discussed including two new types of recirculating-delay-line test fixture. The most important performance parameters may be obtained in a convenient way from the signature of these devices.

References

1. M. K. Barnoski and S. M. Jensen, "Fiber Waveguides: A Novel Technique for Investigating Attenuation Characteristics," Appl. Opt. **15,** 2112 (1976).
2. S. D. Personick, "Photon Probe—An Optical Time-Domain Reflectometer," Bell Syst. Tech. J. **56,** 355 (1977).
3. F. P. Kapron and P. D. Lazay, "Monomode Fiber Measurement Techniques and Standards," Proc. Soc. Photo-Opt. Instrum. Eng. **425,** 40 (1983).
4. B. Costa, F. Esposto, C. D'Orio, and P. Morra, "Splice Loss Evaluation by Means of the Backscattering Technique," Electron. Lett. **15,** 550 (1979).
5. P. Matthijsse and C. M. DeBlok, "Field Measurement of Splice Loss Applying the Backscattering Method," Electron. Lett. **15,** 795 (1979).
6. A. Le Boutet, "Analysis of Backscattering Results Applied to Cable Connection," in *Technical Digest, Fifth European Conference on Optical Communication, Amsterdam* (1979).
7. D. Rittich, "Low Loss Optical Couplers," in *Advances in Ceramics, Vol. 2* (American Ceramic Society, Columbus, Ohio, 1981), pp. 451–462.
8. B. Costa, B. Sordo, U. Menaglia, L. Piccari, and G. Grasso, "Attenuation Measurements Performed by Backscattering Technique," Electron. Lett. **16,** 352 (1980).
9. M. D. Rourke, "Measurement of the Insertion Loss of a Single Microbend," Opt. Lett. **6,** 440 (1981).
10. M. Eriksrud and A. R. Mickelson, "Application of the Backscattering Technique to the Determination of Parameter Fluctuations in Multimode Optical Fibers," IEEE J. Quantum Electron. **QE-18,** 1478 (1982).
11. B. L. Danielson, "Backscatter Measurements on Optical Fibers," Natl. Bur. Stand. U.S. Tech. Note 1034 (1981).
12. S. M. Jensen, "Observation of Differential Mode Attenuation in Graded-Index Fiber Waveguides Using OTDR," in *Technical Digest, Optical Fiber Communication, Washington, D.C.* (1979).
13. M. K. Barnoski, S. M. Jensen, and M. D. Rourke, "OTDR Differential-Modal-Attenuation Measurements," in *Technical Digest, Fourth European Conference on Optical Communication, Genoa* (1978).
14. L. Stensland and G. Borak, "Raman Time-Domain Reflectometry," in *Technical Digest, Third International Conference on Integrated Optics and Optical Fiber Communication* (Optical Society of America, Washington, D.C., 1981, paper WF1.
15. M. Biet and J. P. Pochelle, "Backscattering Analysis of Optical Fibers in the Dual Mode Regime," J. Opt. Commun. **4,** 42 (1983).
16. O. I. Szentesi, "Field Measurements of Optical Fiber Cable Systems," in *Technical Digest, Symposium on Optical Fiber Measurements,* Boulder, Colo. (1980), pp. 37–42.
17. J. Hecht, "Fiberoptic Test Equipment Survey," Lasers Appl. **2,** 63 (1983).
18. E. Brinkmeyer, "Analysis of the Backscatter Method for Single-Mode Optical Fibers," J. Opt. Soc. Am. **70,** 1010 (1980).
19. E. G. Neumann, "Analysis of the Backscattering Method for Testing Optical Fiber Cables," Electron. Commun. (AEU) **34,** 157 (1980).

20. For precise definitions of these quantities, see A. G. Hanson, *Optical Waveguide Communications Glossary*, Natl. Bur. Stand. U.S. Handbook 140 (1982).
21. A. H. Hartog and M. P. Gold, "On the Theory of Backscattering in Single-Mode Optical Fibers," IEEE/OSA J. Lightwave Technol. **LT-2,** 76 (1984).
22. J. L. Hullett and R. D. Jeffery, "Long-Range Optical Fiber Backscatter Loss Signatures Using Two-Point Processing," Opt. Quantum Electron. **14,** 41 (1982).
23. J. Kurki and J. Viljanen, "A High Performance Backscattering Set-Up Using Multimode Light Channels," Opt. Quantum Electron. **15,** 471 (1983).
24. B. Costa, B. Sordo, and E. Vezzoni, "High Dynamic Range Backscattering Measurements," in *Advances in Ceramics, Vol. 2* (American Ceramic Society, Columbus, Ohio, 1981), pp. 273–277.
25. K. Okada, "Backscattering Measurement," in *Annual Reviews in Electronics, Computers, and Telecommunications, Vol. 3* (Ohm Publishing, Tokyo, 1982), pp. 299–313.
26. D. A. Philen, I. A. White, J. F. Kuhl, and S. C. Mettler, "Single-Mode Fiber OTDR: Experiment and Theory," IEEE J. Quantum Electron. **QE-18,** 1499 (1982).
27. A. H. Hartog, "Advances in Optical Time-Domain Reflectometry," in *Technical Digest, Symposium on Optical Fiber Measurements*, Boulder, Colo. (1984), pp. 89–94.
28. D. Marcuse, *Principles of Optical Fiber Measurements* (Academic, New York, 1981), Chap. 5.
29. B. L. Danielson, "Backscatter Signature Simulations," Natl. Bur. Stand. U.S. Tech Note 1050 (1981).
30. Ref. 28, p. 240.
31. M. I. Skolnik, *Introduction to Radar Systems* (McGraw-Hill, New York, 1962), p. 464.
32. R. D. Jeffery and J. L. Hullett, "N-Point Processing of Optical Fiber Backscatter Signals," Electron. Lett. **16,** 822 (1982).
33. "Standard Optical Waveguide Fiber Material Classes and Preferred Sizes," EIA Document RS-458A (1984).
34. M. K. Barnoski, "Coupling Components for Optical Fiber Waveguides," in *Fundamentals of Optical Fiber Communications* (Academic, New York, 1981), Chap. 3. In the case of bulk-optic directional couplers where the source is imaged onto the fiber end, the injected power may be independent of $2a$ for diffraction-limited laser sources and approximately proportional to $2a$ for semiconductor lasers with a stripe geometry emitting surface. However, Murata[35] finds that coupled power in the latter case is largely independent of core diameter.
35. H. Murata, S. Inaco, Y. Matsuda, and T. Kuroha, "Optimum Design for Optical Fiber Used in Optical Cable System," in *Technical Digest, Sixth European Conference on Optical Communications, York* (1980).
36. A. H. Cherin, E. D. Head, C. R. Lovelace, and W. B. Gardner, "Selection of Mandrel Wrap Mode Filters for Optical Fiber Loss Measurements," Fiber Int. Opt. **4,** 49 (1982).
37. J. L. Hullett and R. D. Jeffery, "Long-Range Optical Fiber Backscatter Loss Signatures Using Two-Point Processing," Opt. Quantum Electron. **14,** 41 (1982).
38. M. Gold, "Design of a Long-Range Single-Mode OTDR," IEEE/OSA J. Lightwave Technol. **LT-3,** 39 (1985).
39. M. Eriksrud, unpublished work.
40. L. G. Cohen, "Shuttle Pulse Measurements of Pulse Spreading in an Optical Fiber," Appl. Opt. **14,** 1351 (1975).
41. D. Marcuse, "Steady-State Losses of Optical Fibers and Fiber Resonators," Bell. Syst. Tech. J. **55,** 1445 (1976).
42. S. A. Newton, J. E. Bowers, and H. J. Shaw, "Single-Mode Fiber Recirculating Delay Line," Proc. Soc. Photo-Opt. Instrum. Eng. **326,** 108 (1982).
43. F. T. Stone, W. B. Gardner, and C. R. Lovelace, "Calorimetric Measurement of Absorption and Scattering Losses in Optical Fibers," Opt. Lett. **2,** 48 (1978).
44. K. Inada, "A New Graphical Method Relating to Optical Fiber Attenuation," Opt. Commun. **19,** 437 (1976).
45. E. G. Neumann, "Optical Time-Domain Reflectometer: Comment," Appl. Opt. **17,** 1675 (1978).
46. M. P. Gold and A. H. Hartog, "Measurement of Backscatter Factor in Single-Mode Fibers," Electron. Lett. **17,** 965 (1981).
47. C. H. Hudson, "NBS Standard Reference Materials Catalog 1984–85," Natl. Bur. Stand. U.S. Spec. Publ. 260 (1984).
48. "The Role of Standard Reference Materials in Measurement Systems," Natl. Bur. Stand. U.S. Monogr. 148 (1975).